RESEARCH ARTICLE OPEN ACCESS

Simulation Of Wind-Hydro Microgrid for Rural Energy System

P.Bhaskara Prasad[1],N.Sireesha[2],H.Karthik[3],P.Jyothsna[4],A.Vamshidhar Reddy[5]
1(Assistant Professor, Electrical and Electronics Engineering , Annamacharya Institute of Technology and Sciences,Rajampet
Email: Bhaskara.papugari@gmail.com)
2,3,4,5 (UG Student,Electrical and Electroincs Engineering, Annamacharya Institute of Technology and Sciences , Rajampet
Email: narasireesha6@gmail.com)

Abstract:
This work deals with a renewable energy based microgrid (MG) for standalone operation. The places, where renewable energy sources such as wind, solar, hydro, etc., are in abundance, use them to generate electricity by developing wind–hydro based MG. The main control unit of MG is voltage source inverter (VSI) in which an indirect current control is applied. This VSI is used for power quality improvements through harmonics suppression of nonlinear loads; voltage regulation during contingencies such as load unbalance; and reactive power compensation at point of common coupling according to the system requirement. It is capable of providing power balance under various changes among the generation, storage, and demand units. For appropriate functioning of VSI, a reweighted zero attractor least mean square control algorithm is applied to generate pulsewidth modulation switching pulses for VSI. A model of MG is developed in MATLAB/Simulink environment to simulate its performance in normal and dynamic conditions at linear and nonlinear loads.

Keywords — **Battery bank, power quality, reweighted zero attractor least mean square (RZALMS), synchronous reluctance generator (SyRG), wind–hydro microgrid (MG).**

I. INTRODUCTION

The electric power is provided to the remote places either by DG sets or available renewable resources such as wind, hydro, solar, etc. The DG sets impose cost on remote applications and lifestyle becomes expensive though the renewable resources are economic in generation but are very unreliable as their generations are season dependent. Therefore, the combinations of renewable resources can be a promising technology to attain the reliability.In photovoltaic systems are investigated with various control schemes. Such systems consist of dc–dc and dc–ac converters. Another combination of converters is called hybrid converters having switching between converters. A hybrid MG is reported in with wind and diesel resources. In such MG droop control is utilized for the frequency regulation of an ac bus. In a
renewable MG for energy management is reported having configuration with two converters, one is ac–power flow. While in the proposed work, a single voltage source inverter (VSI) (dc–ac converter) as the control unit and one dc-dc converter is utilized for maximum power tracking (MPPT).
of nonlinear loads, voltage regulation at load variations, reactive power compensation based on system requirement. It also manages balanced power flow among various units, i.e., wind–hydro generators, the battery storage, and loads.

The main contribution of the paper is as follows.

1) A single VSI control based MG is developed. Moreover, the wind power of PMBLDCG is converted into dc power using a diode rectifier. Therefore, this topology has reduced the overall cost of the system.
2) The PMBLDCG does not need sensors such as speed sensor, position sensor, and wind speed sensor for MPPT control, thus further reducing the cost.
3) An RZALMS control approach is implemented in the MG VSI for fast responses during steady-state and dynamic conditions.
4) Generators used are maintenance free and having high efficiency.

II. MG CONFIGURATION AND CONTRO STRATEGY

Fig. 1 depicts the renewable-based MG comprising of hydro and wind sources. The hydro power is generated using SyRG, a constant power generator and this power is fed to the ac loads. The PMBLDCG is used to generate the electricity from windpower at variable speeds and a diode rectifier is used to convert it into dc power, which is fed to the boost converter for MPPT using the P&O control technique. This extracted power

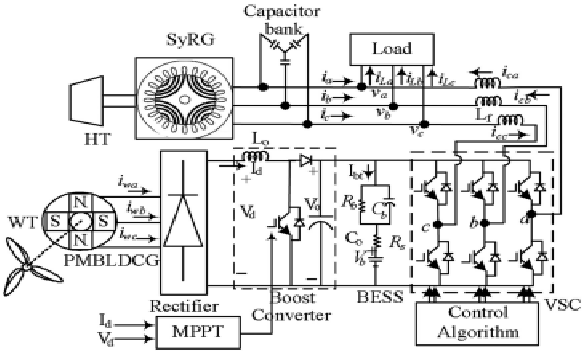

Fig. 1.Wind–hydro MG configuration

is delivered to the ac loads through a VSI and excess generated power is stored in the battery bank connected parallel to the VSI. This VSI is connected to the hydro power generator (SyRG) and loads at point of common coupling (PCC) through interfacing inductors (L_f). A capacitor bank is connected at SyRG terminals to support reactive power to MG for voltage buildup. The design data of the proposed MG are given in Appendix.

To operate MG in satisfactory manner, it must provide good quality power as regulated sinusoidal voltage and frequency.

The RZALMS approach is used to estimate the active load power current component from the load current at (x)th sample

This work presents MG performance with an RZALMS Fig. 2.

Fig.2.MG control approach control approach

The underpin a zero attractor for differentiating between zero taps and nonzero taps, as shown in Fig. 2.

The parameters μ (step size), i_{La} (phase "a" load current), u_{pa} (in-phase template), u_{qa} (quadrature template), σ and ψ (small constants) are used in the control approach.

Phase voltages are computed from line voltages as [25], [26]

$$v_a = 1/3(2v_{ab} + v_{bc}) \quad (1)$$

$$v_b = 1/3(-v_{ab} + v_{bc}) \quad (2)$$

$$v_c = 1/3(-v_{ab} - 2v_{bc}). \quad (3)$$

The terminal voltage V_t is derived from phase voltages as

$$V_t = \sqrt{\left(2\left(v_a^2 + v_b^2 + v_c^2\right)/3\right)}. \quad (4)$$

In-phase template of phase "a" voltage as

$$u_{pa} = v_a/V_t. \quad (5)$$

Similarly, other two in-phase templates for phase "b and c" (u_{pb}, u_{pc}) are also achieved.

The quadrature voltage templates of three-phase voltages are as follows:

$$u_{qa} = (-u_{pa} + u_{pc})/\sqrt{3} \quad (6)$$

$$u_{qb} = (3u_{pa} + u_{pb} - u_{pc})/\sqrt{3} \quad (7)$$

$$u_{qc} = (-3u_{pa} + u_{pb} - u_{pc})/\sqrt{3}. \quad (8)$$

ipa (x) = ipa (x − 1) + μu pa epa − σsign(ipa (x − 1)) 1 + ψ |ipa (x − 1)| . (9)

The lesser magnitudes taps are specifically shrank by RZALMS. The reweighted zero attractor impacts only those taps for which magnitudes are comparable to 1/ψ and there is

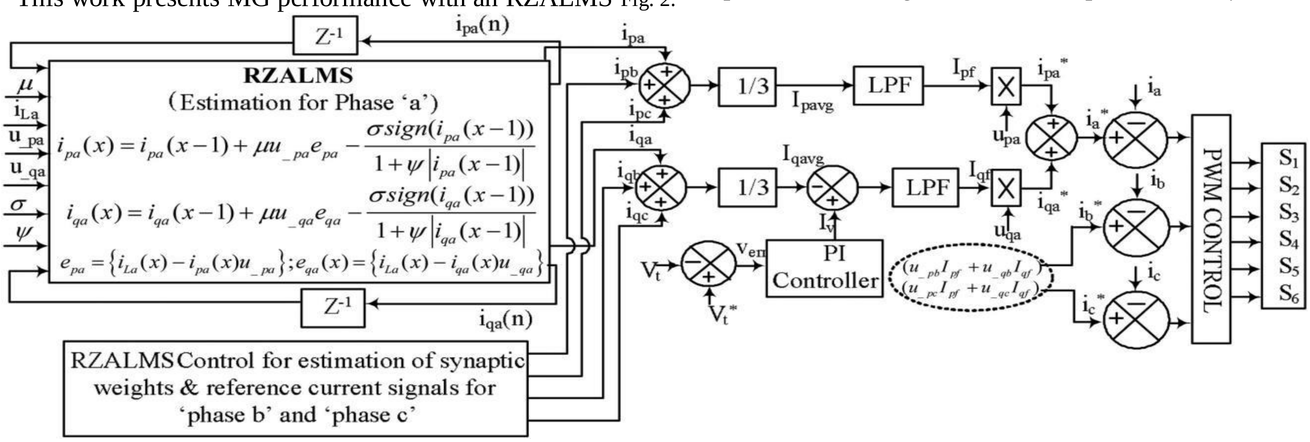

little shrinkage used on the taps whose |ipa (x–1)| >> 1/ψ. In this way, the bias of RZALMS can be reduced.
The error between desired and actual outputs epa (x) at xth sample is calculated as
epa (x) = {iLa (x) − ipa (x) u pa } . (10)
Similarly, the active load power components of other two phases (b, c) are computed from the RZALMS approach. The reactive load power current component from the load current at (x)th sample for phase "a" is computed as iq
a (x) = iq a (x − 1) + μu q a eq a − σsign(iq a (x − 1)) 1 + ψ |iq a (x − 1)| (11)

$$e_{qa}(x) = \{i_{La}(x) - i_{qa}(x)u_{qa}\}. \quad (12)$$

Similarly, the reactive load power current components of other two phases (*b*, *c*) are also achieved using the same approach.

The values of μ, σ, and ψ are selected as 0.015, 0.0005, and 10, respectively.
The equivalent per phase of load active power current component is derived as

.

After passing through a low-pass filter (LPF), this component is expressed as the active power current

$$I_{pavg} = \frac{i_{pa} + i_{pb} + i_{pc}}{3} \quad (13)$$

component of source current (I_{pf}).

The equivalent per phase of reactive load power current component is generated as

$$I_{qavg} = \frac{i_{qa} + i_{qb} + i_{qc}}{3}. \quad (14)$$

To regulate PCC voltage, a Proportional and Integral (PI) voltage controller is used with the gain values of k_p and k_i. The error between the reference terminal voltage (V^*_t) and the sensed PCC voltage (V_t) is fed to a PI controller, and its output is estimated as

$$I_v(x) = I_v(x-1) + k_p\{V_{err}(x) - V_{err}(x-1)\} + k_i V_{err}(x) \quad (15)$$

where V err is the voltage error and it is expressed as

V err = V ∗ t − V t. (16)

The reactive component of the source current is estimated as

Iq t = I v − Iqavg . (17)

extracting it from an LPF, it is said the reactive power component Iqf .

The active and reactive power components of reference threephase source currents are calculated as

i ∗ pa = Ipf u pa i ∗ pb = Ipf u pb i ∗ pc = Ipf u pc (18)

i ∗ q a = Iqf u q a i ∗ q b = Iqf u q b i ∗ q c = Iqf u q c . (19)

The reference three-phase source currents are estimated as

i ∗ a = i ∗ pa + i ∗ q a i ∗ b = i ∗ pb + i ∗ q b i ∗ c = i ∗ pc + i ∗ q c . (20)

To generate PWM pulses for switching to three legs of VSI, these reference source currents (i ∗ a , i ∗ b , i ∗ c) are compared with the sensed three-phase source currents (ia , ib , ic)

III . RESULTS AND DISCUSSION

Simulated results of MG are demonstrated in this section. Steady-state and dynamic responses of a renewable-based MG are shown and the behavior of intermediate signals of control approach at load unbalancing is depicted in detail. The wind MPPT using the P&O approach is also included.

A. MPPT of Wind Power

The MPPT of wind generation is achieved through applying a P&O approach. It is shown in Fig. 3 that at the wind speed variation, the PMBLDCG current of phase "a" is also reduced.

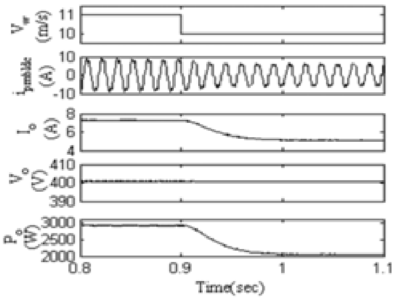

Fig. 3. P&O approach based MPPT.

B. Response of RZALMS Control Approach at Linear and Nonlinear Loads

The performance of wind–hydro based MG depends on its control approach robustness. To demonstrate satisfactory response of the control approach, its various intermediate signals are depicted in Fig. 4 at nonlinear loads. The load unbalance is created at t = 1.3 s, and the load on that phase is recovered at t = 1.4 s.

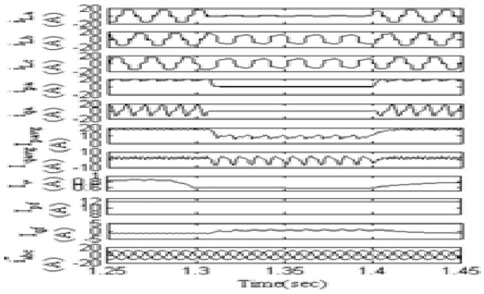

Fig. 4. Intermediate signals of RZALMS control algorithm at nonlinear load.

power balance in the MG during various states such as high wind power generation, load unbalancing, and peak load demand. Such MG provides energy independence in rural areas and contributes in reducing the fossil consumption its bad impact on the environment. A single VSI has performed power quality improvement and power balancing. The PMBLDCG does not require speed sensor, position sensor, and wind speed sensor for MPPT control. Individual inverters and converters are not being used on various units viz., wind, hydro, battery bank, etc. Therefore, the overall system cost and maintenance is reduced 1) Ratings of SyRG: Three-phase, 3.7 kW, 230 V, 1500 r/min. 2) Ratings of PMBLDCG: Three-phase, 230 V, 3.7 kW, 1500 r/min. 3) Battery Rating: 396 V, 2.778 kWh (33 Cells of 12 V, 7 Ah). 4) PI controller Gains for voltage controller: kp = 0.4, and ki = 0.08. 5) Interfacing inductance Lf = 3.5 mH, Capacitor Bank = 8 kvar.

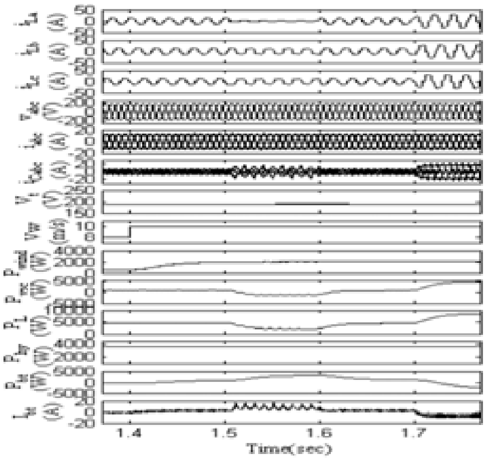

Fig. 5. Performance of MG under dynamic condition at nonlinear load.

C.Dynamic Behavior of Wind–Hydro Based MG The dynamic performance of wind–hydro based MG under different scenarios is illustrated in Fig. 5 at nonlinear load. At t = 1.4 s, the wind speed is increased, accordingly the wind power (Pwind) is also increased. The load demand (PL) and hydro generation (Phy) are fixed, therefore, increased.

IV. CONCLUSION

A renewable wind–hydro based MG has been developed. The performance of MG has been demonstrated using RZALMS control approach to provide power quality solutions, i.e., harmonics suppression, reactive power compensation, load balancing, and voltage control. It has also managed the power balance in the MG during various states such as high wind power generation, load unbalancing, and peak load demand. Such MG provides energy independence in rural areas and contributes in reducing the fossil consumption and its bad impact on the environment. A single VSI has performed power quality improvement and power balancing. The PMBLDCG does not require speed sensor, position sensor, and wind speed sensor for MPPT control. Individual inverters and converters are not being used on various units viz., wind, hydro, battery bank, etc. Therefore, the overall system cost and maintenance is reduced.

V. REFERENCES

[1] A. Rashid, N. Hasan, K. T. Parvez, and M. N. I. Maruf, "Study and analysis of a small scale micro-grid using renewable energy resources," in Proc. Int. Conf. Elect. Eng. Inf. Commun. Technol., Dhaka, Bangladesh, 2015, pp. 1–4.

[2] M. S. Mahmoud, M. Saif Ur Rahman, and F. M. A. L. Sunni, "Review of microgrid architectures – a system of systems perspective," IET Renewable Power Gener., vol. 9, no. 8, pp. 1064–1078, 2015.

[3] S. V. Cotto and W.-J. Lee, "Microgrid modular design for tribal healthcare facilities: Kayenta health center PV system case study" IEEE Trans. Ind. Appl., vol. 53, no. 6, pp. 5121–5129, Nov./Dec. 2017

[4] T. Ma, M. H. Cintuglu, and O. A. Mohammed, "Control of a hybrid AC/DC microgrid involving energy storage and pulsed loads," IEEE Trans. Ind. Appl., vol. 53, no.1, pp. 567–575, Jan./Feb. 2017.

[5] K. Sun, X. Wang, Y. W. Li, F. Nejabatkhah, Y. Mei, and X. Lu, "Parallel operation of bidirectional interfacing converters in a hybrid AC/DC microgrid under unbalanced grid voltage conditions," IEEE Trans. Power Electron., vol. 32, no. 3, pp. 1872–1884, Mar. 2017.

[6] F. Cingoz, A. Elrayyah, and Y. Sozer, "Optimized settings of droop parameters using stochastic load modeling for effective DC microgrids operation," IEEE Trans. Ind. Appl., vol. 53, no. 2, pp. 1358–1371, Mar./Apr. 2017.

[7] G. Pathak, B. Singh, and B. K. Panigrahi, "Three-phase four-wire winddiesel based microgrid," in Proc. IEEE 6th Int. Conf. Power Syst., 2016, pp. 1–6.

[8] World Energy Resources 2013 Survey, 2013. [Online]. Available: https://www.worldenergy.org/wp-ontent/2013/Complete_WER_2013 _Survey.

[9] N. Bauer et al., "Global fossil energy markets and climate change mitigation: An analysis with REMIND," Climatic Change, vol. 136, pp. 69–82, 2013.

[10] F. P. Perera, "Multiple threats to child health from fossil fuel combustion: Impacts of air pollution and climate change,"Environ. Health Perspectives, vol. 136, pp. 69–82, 2016

[11] B. Atilgan and A. Azapagic, "Life cycle environmental impacts of electricity from fossil fuels in Turkey," J. Cleaner Prod., vol. 106, pp. 555–564, 2015.

[12] F. Blaabjerg, Y. Yang, and K. Ma, "Power electronics - key technology for renewable energy systems - status and future," in Proc. 3rd Int.Conf. Elect. Power Energy Convers. Syst., Istanbul, Turkey, 2013, pp. 1–6.

[13] B. K. Bose, "Global energy scenario and impact of power electronics in 21st century," IEEE Trans. Ind. Electron., vol. 60, no. 7, pp. 2638–2651, Jul. 2013.

[9] N. Bauer et al., "Global fossil energy markets and climate change mitigation: An analysis with REMIND," Climatic Change, vol. 136, pp. 69–82, 2013.

[14] Y. S. Elrayyah and M. Elbuluk, "Microgrid-connected PV-based sources: A novel autonomous control method for maintaining maximum power," IEEE Ind. Appl. Mag., vol. 21, no. 2, pp. 19–29, Mar./Apr. 2015.

[15] R. Engleitner, A. Nied, M. S. M. Cavalca, and J. P. da Costa, "Dynamic analysis of small wind turbines frequency support capability in a lowpower wind-diesel microgrid," IEEE Trans. Ind. Appl., vol. 54, no. 1, pp. 102–111, Jan./Feb. 2018.

[16] A. Merabet, K. Tawfique Ahmed, H. Ibrahim, R. Beguenane, and A. M. Y. M. Ghias, "Energy management and control system for laboratory scale microgrid based wind-PV-battery," IEEE Trans. Sustain. Energy, vol. 8, no. 1, pp. 145–154, Jan. 2017.

[17] U. K. Kalla, B. Singh, and S. S. Murthy, "Modified electronic load controller for constant frequency operation with voltage regulation of small hydro-driven single-phase SEIG," IEEE Trans. Ind. Appl., vol. 52, no. 4, pp. 2789–2800, Jul./Aug. 2016.

[18] M. Rezkallah, A. Chandra, B. Singh, and S. Singh, "Microgrid: Configurations, control and applications,